



Research article

Ozone formation in relation with combustion processes in highly populated urban areas

Pasquale Avino * and Maurizio Manigrasso

DIT, INAIL settore Ricerca, via IV Novembre 144, I-00187 Rome, Italy

* **Correspondence:** Email: p.avino@inail.it; Tel: +39-06-9789-2611;
Fax: +39-06-9789-1.

Abstract: The complex chain of photochemical reactions is one of the most important tasks in the air quality evaluation, especially in urban areas. In fact, in this case there are high emission levels of NO_x and no-methane hydrocarbons by combustion processes such as automotive traffic, domestic heating and industrial plants. Ozone is not emitted directly into the atmosphere but it is formed from a complex series of reactions between emitted nitrogen oxides (NO_x) and reactive organic compounds (ROC). The high ozone concentrations, which occur during photochemical episodes, are usually accompanied by elevated concentrations of other photochemical oxidants such as nitric acid (HNO₃), peroxyacetyl nitrates (PANs), hydrogen peroxide (H₂O₂), etc. The complex series of these reactions constitutes the most important issue to the degradation of air quality. Further, the NMHCs play a key role in the formation of photochemical air pollution: they are considered as precursors for ozone production at the ground level when the sunlight and nitrogen oxides are present. From a practical point of view defining a quality standard or a limit is substantially correct but it is not sufficient to solve the problem. So it should become necessary to acquire knowledge on the different formation mechanisms of the photochemical pollution phenomena. In this paper there will be shown the results of a long-term study performed in Rome for evaluating the ozone formation in relationship with the automotive traffic density.

Keywords: ozone; NO₂; photochemical process; incomplete combustion; formaldehyde; primary pollutants; secondary pollutants; NMHCs; elemental carbon; radon

1. Introduction

Ozone, an atmospheric gaseous secondary pollutant, is formed through the reaction of O₂ with

atomic oxygen deriving from the photolysis of NO_2 (Figure 1).

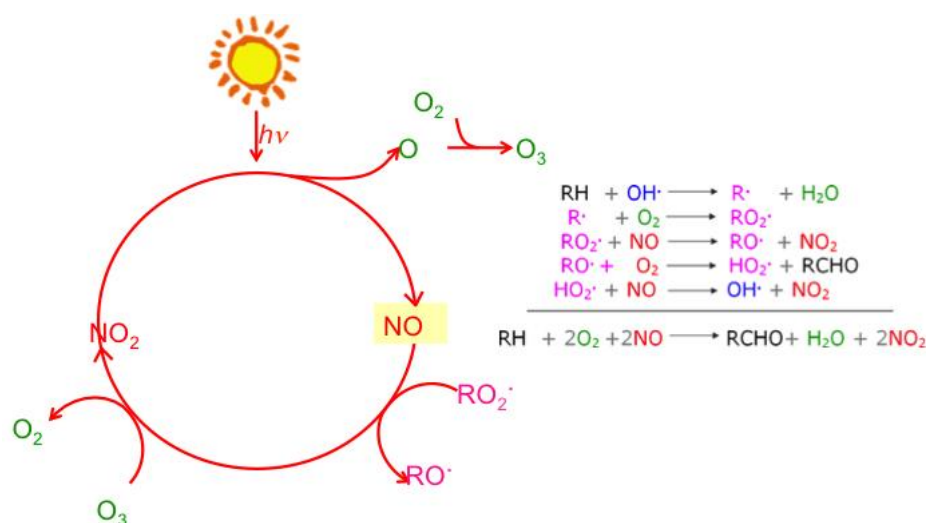


Figure 1. Reactions occurring during atmospheric radical activity: photochemical smog episode.

In the radical chain reaction, NO_2 is produced through the oxidation of NO by O_3 and the radical RO_2 and HO_2 [1]. No O_3 accumulation would occur if the formation of NO_2 were due only to the reaction of O_3 with NO . In this case, NO_2 and O_3 show a complementary pattern of variation: maximum values of O_3 corresponds to minimum values of NO_2 and vice versa. However, in the case of intense pollution episodes, in presence of both reactive hydrocarbons and OH radicals [2], the RO_2 and HO_2 radicals that are formed oxidize NO and cause O_3 accumulation.

OH governs atmospheric chemistry during the day since its formation depends on radiation from the Sun [2-5]. The initial reaction involves the photolysis of ozone by solar radiation. The oxygen atom formed then reacts with water to form OH . Other OH sources include the photolysis of nitrous acid (HNO_2), hydrogen peroxide (H_2O_2) or peroxy-methane (CH_3OOH) the reaction of nitrogen monoxide (NO) with the hydroperoxy radical (HO_2), the reaction of alkenes with ozone and the HCHO , ClNO_2 photolysis [6-18].

Among the many important roles played by ozone in atmosphere, a very important part one involves the generation of OH radicals, which are responsible for initiating the oxidation of a wide variety of atmospheric trace constituents. The OH production occurs dominantly from the formation of the excited $\text{O}(^1\text{D})$ species in the UV photolysis of ozone, followed by the reaction of $\text{O}(^1\text{D})$ with H_2O vapor.

OH radicals also derive from photolysis of HCHO in presence of NO [19,20], from the ozonolysis reaction of alkenes [5,21-25] and from the ClNO_2 photolysis [26]. For more detail, Mao et al. [27] calculated the relative importance of the above sources of OH in New York and estimated HNO_2 photolysis contributed up to 60%.

Different authors deeply investigated the species involved in the atmospheric oxidation capacity [22,28] such as O_3 , OH , NO_3 : in their experimental conditions they found the average oxidation capacity of OH , O_3 and NO_3 radicals through the entire day to be 89.4, 10.3 and 0.3% of the total oxidation capacity, respectively, with different partial contribution during the daytime and nighttime.

Taking into account the photochemical processes leading to the ozone formation, the Directive

2008/50/EC [29] requires the measurement of the ozone precursors that are defined as “substances which contribute to the formation of ground-level ozone”. In urban areas, at least one measuring station is to be installed to supply data on O₃ precursors.

The directive recommends the measurements of Non-Methane Hydrocarbons (NMHCs), such as Acetylene, Ethane, Ethylene, Propane, Propene, *n*-Butane, *i*-Butane, 1-Butene, *trans*-2-Butene, *cis*-2-Butene, 1,3-Butadiene, *n*-Pentane, *i*-Pentane, 1-Pentene, 2-Pentene, Isoprene, *n*-Hexane, *i*-Hexane, *n*-Heptane, *n*-Octane, *i*-Octane, Benzene, Toluene, Ethyl benzene, *m+p*-Xylene, *o*-Xylene, 1,2,4-Trimethylbenzene, 1,2,3-Trimethylbenzene, 1,3,5-Trimethylbenzene, Formaldehyde, Total Non-Methane Hydrocarbons (T-NMHCs). An important parameter is the “incremental reactivity” to quantify ozone impacts of NMHCs. This is defined as the change on ozone caused by adding an arbitrarily small amount of the test NMHC to the emissions in the episode, divided by the amount of test NMHC added. This can also be thought of as the partial derivative of ozone with respect to emissions of the NMHC.

The rate of ozone increase caused by these processes is dependent on the amounts of NMHCs present, the rate constants for the NMHC’s initial reactions, and the level of OH radicals and other species with which the NMHCs might react. Ozone production continues as long as sufficient NO_x is present that reactions of peroxy radicals (RO₂) with NO_x compete effectively with their reactions with other peroxy radicals. It should be noted that the OH radical levels are particularly important in affecting the O₃ formation rate in the presence of NO_x because reaction with OH is a major (and in many cases the only) process causing most NMHCs to react.

Ozone effects on human health are mainly attributed to its reactions, particularly the ozonization of lipids [30,31]. The plasmatic membrane is the cellular component mainly damaged [32].

Impairment of the pulmonary function is the principal effect observed [33]. The susceptible subpopulations can be identified in children. Children represent for several reasons a very sensitive group of the population. In comparison with adults, children have a higher intake of ozone and other air pollutants. This is due to a higher basal metabolic rate, resulting both in higher breath volume per minute and higher breathing frequency. Further, their respiratory tract is still under development until six years old, and is therefore more susceptible to the inflammatory effects of ozone. It should also be considered that children’s immune systems are not yet fully developed either and are generally under bigger stress. For these and other reasons, children are at higher risk concerning exposure to ambient ozone concentrations.

Patients with lung disease and smokers are thought to be at increased risk of ozone-induced decrements in lung function because an equivalent decrement in lung function would have more serious health consequences given their already compromised lung function [34].

Asthma patients are considered an important risk population because some 5–10% of the general population suffer from asthma. Asthma encompasses clinical conditions that include airflow limitation (obstruction) and (chronic) inflammation of the airways. Due to the irritant nature of ozone, capable of inducing airway inflammation and bronchoconstriction, asthma patients are deemed to be at enhanced risk from exposure to ozone and photochemical ‘smog’, because inflamed airways contribute to the pathogenesis and exacerbation of the disease and to morbidity and mortality for asthma.

In addition, it is now clearly recognized that ozone at ambient concentrations found in Europe can cause a range of effects including visible leaf injury, growth and yield reductions [35]. Moreover, being ozone a secondary pollutant with a regional distribution, these effects may occur over large areas of rural Europe.

Consistently, the European Directive 2008/50/EC [29] fixes limits not only for the protection of

the human health, but also for the protection of vegetation. This Directive establishes long-term objectives, target values, alert threshold and information threshold for concentrations of ozone in ambient air in the Community, designed to avoid, prevent or reduce harmful effects on human health and the environment as a whole:

- ✓ “target value” are fixed values, in the long term, to avoid harmful effects on human health and/or the environment as a whole, to be attained where possible over a given period;
- ✓ “long-term objective” are fixed in order to avoid, according to current scientific knowledge, direct adverse effects on human health and/or the environment as a whole are unlikely. This objective is to be attained in the long term, save where not achievable through proportionate measures, with the aim of providing effective protection of human health and the environment;
- ✓ “information threshold” refers to a level beyond which there is a risk to human health from brief exposure for particularly sensitive sections of the population and at which up-to-date information is necessary;
- ✓ “alert threshold” refers to a level beyond which there is a risk to human health from brief exposure for the general population and at which immediate steps shall be taken by the Member States.

In this paper, we discuss the photochemical processes occurring in highly populated and anthropogenic urban areas with particular interest in the smog formation and the NMHC contribution to the ozone levels. In particular, we calculate the contribution in percentage of each determined NMHC to the ozone formation in downtown a big urban area such as Rome, comparing these values with other data reported in literature.

2. Materials and Method

2.1. Sampling site

The gaseous and aerosol sampling and measurements were carried out in downtown Rome at the INAIL’s building: the sampling point is located at 40 m about the ground level. The sampling location has been chosen in open fields but in a very high traffic zone (high density of automotive and heavy traffic, e.g. cars, buses, coaches, etc.) and in a populated area (e.g., domestic heating, cooking activity): the anthropogenic emissions result the major pollution in such area. The measurements reported in this paper cover a long-time period ranging between the ‘90s until December 2014.

2.2. Primary and secondary pollutants: measuring equipment

As regards the traditional atmospheric pollutants like ozone, nitrogen dioxide, nitrous acid, formaldehyde, benzene and toluene, we will also show data referring to the sequence of ten year of measurements, from 1991 to 2000, taken in downtown Rome at ground level.

Gaseous primary and/or secondary pollutants were measured by means of Differential Optical Absorption Spectroscopy (DOAS, mod. AR 500, Opsis, Sweden) [36-38]. The DOAS system consists of an emitter (a xenon lamp at high pressure), a receiver, a spectrophotometer equipped with an optical fiber and a computer for the system management (data elaboration and storage). The absorption spectra of each monitored chemical species are acquired at their relative typical wavelength ranges. The distance between emitter and receiver is about 280 m: this parameter is important because it influences the sensitivity of the measures. The absorbance of light from the emitter is continuously

measured within the wavelength range 240–350 nm to determine several compounds. The air pollutant concentrations are automatically calculated from the absorbance values, in accordance with Lambert-Beer's law. The DOAS technique offers the possibility of simultaneous measurements of primary and secondary air pollutants concentration by averaging them on a long optical path ranging up to some km, that as such represent the average pollution level better than classical point source analyzers.

All the particulate matter samplings were performed by means of a 10 μm sampling head. The EC and OC separation was carried out by means of an Ambient Carbon Particulate Monitor 5400 (ACPM 5400, Rupprecht & Patashnik Co Inc., Albany, NY, USA) based on a two-step combustion procedure (Figure 2).

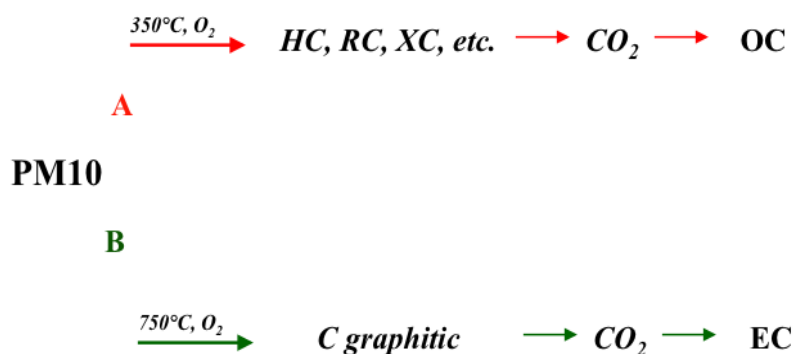


Figure 2. Thermal method for the separation of Organic Carbon and Elemental Carbon.

By means of a non-dispersive infrared detector (NDIR) the instrument measures the CO_2 amount released when a particulate matter sample collected in a collector is oxidized at elevated temperatures [39,40]. The temperature of the collector is raised to 350 $^\circ\text{C}$ for a period of 13 min during which the instrument measures the CO_2 concentrations in the analysis loop. Then, a final burn of 8 min at 750 $^\circ\text{C}$ takes place to burn off the high-temperature carbon that was not oxidized at 350 $^\circ\text{C}$. The instrument measures the OC concentration at 350 $^\circ\text{C}$ and the TC concentration at the 750 $^\circ\text{C}$ step. Finally, the EC is calculated as the difference of TC and OC [41].

The PM_{10} was monitored by means of a Tapered Element Oscillating Microbalance (TEOM) Ambient Particulate Monitor (R&P). The instrument uses a vibrating collection substrate to collect the particles. The change in sample mass causes the change of the frequency of oscillation that is used to calculate the mass concentration.

The Radon concentration was measured by a PBL Mixing Monitor (FAI Instruments, Fonte Nuova, Rome, Italy) [42]. The instrument samples atmospheric PM on 47-mm membrane filters: a Geiger detector measures the β -radioactivity of short-lived decay products of Radon with 1 h time resolution [43-45].

For NMHCs data are based on 36 samples collected in downtown Rome at ground level, in the location close where the gaseous pollutants are recorded. The sampling was performed by Tedlar bag for 15 min in an interval between 07:00 and 13:00 a.m., i.e. the maximum rush time in an urban area. The sampling was carried out for 6 days and every day 6 samples were collected. NMHCs were measured in Rome by means of an automatic GC equipped with FID and PID detectors (columns DB1, 30 m, 0.32 mm ID, 1.8 μm film, and SY-5, 15m, 0.32 mm ID, 1 μm film; cycle time 30 min; temp program 20–90 $^\circ\text{C}$; lowest detection level for benzene 0.4 $\mu\text{g m}^{-3}$); about 30 compounds were investigated.

3. Results and Discussion

The temporal concentration trend of each pollutant can be interpreted using the measurements of the concentrations of natural radioactivity as tracer of the dynamic properties of the atmospheric boundary layer.

The atmospheric primary pollution level is determined by both the intensity of its emissions and the dynamic properties of the atmospheric boundary layer, causing pollutant dilution or accumulation. In this respect, radon and its short-lived decay products can be considered as tracer of the mixing properties of the lower boundary layer, since radon is emitted at a rate that is spatially and temporally constant.

The temporal evolution of Radon concentration can be described by the following equation (Equation 1):

$$\frac{\partial C}{\partial t} = \alpha \Phi_R - \beta \{C_R\} + Adv \quad (1)$$

where C: mixing ratio near the ground; α : parameter which links the mixing properties of the boundary layer with the source intensity; $\Phi_{(R)}$: emission rate of Radon; $\beta \{C_R\}$: term which takes into account the vertical mixing properties of the atmosphere; Adv: advection term. The term $\Phi_{(R)}$ reflects temporal variability of source intensity and the terms α , β and Adv are linked to the dynamics of the lower layers of the atmosphere. The term Adv can be deduced from knowledge of the intensity and direction of the wind at the ground level. The time trend of Radon daughters concentration can be used in order to characterize the terms α and β . In particular, atmospheric stability conditions maximize the first term that takes into account the emission rate of radon, while the 2nd term, accounting for the vertical mixing properties of the atmosphere is negligible. Instead atmospheric instability makes maximum the contribution of such term $\beta \{C_R\}$.

In the decade from 1991 to 2006, the benzene, toluene and SO₂ annual average concentration levels are characterized by clear decreasing trends (Figure 3). For benzene and toluene this is due to a wider diffusion of cars with catalytic converter and it is an effect of a law enacted in 1997 [46], prescribing the limit of 1% benzene concentration in fuels. The same law prescribe that Gasoline Dispensing Facilities must be equipped with vapor recovery equipment to control NMHC emissions during the filling of on-road motor vehicle fuel tanks [47]. In fact, in an urban context dominated by the autovehicular traffic pollution, as downtown Rome, a direct consequence of such legislative decisions was the steady reduction of the benzene emissions. Taking in account this consideration and the frame of measurements determined in Rome [48], it can be understood the overall decline of benzene and toluene annual average concentrations. In particular, for benzene in this decade we assisted to a 60% reduction of its emissions [49].

As regards SO₂, its decreasing trend may be considered as an effect of important European directives, 93/12/CE and 98/70/CE [50], that have imposed, for the decade investigated, and have scheduled, for the next years, considerable reductions of the sulphur content in fuels.

In Figure 4 we can observe that the month averages of benzene, toluene and SO₂ show decreasing values during summer, due both to the lack of contribution of domestic heating and to meteorological conditions characterized by long periods of solar radiation, favoring both the pollutant dispersion due to convective mixing and their photo-oxidation. One-way ANOVA analysis was also performed to compare annual pollutant variations: $p < 0.05$ was considered significant, $p < 0.001$ highly significant. In our case, all the three pollutants, benzene, toluene and SO₂, show significant data ($p < 0.001$).

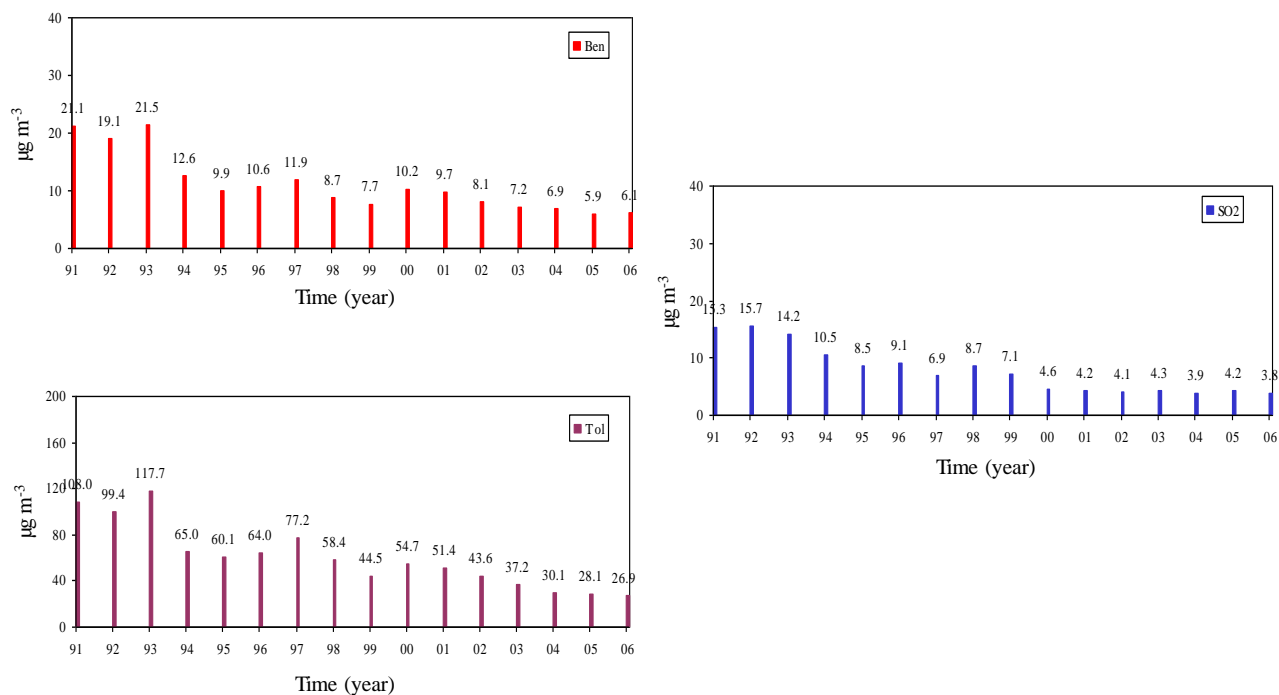


Figure 3. Primary pollutants: annual trends of the month average concentration ($\mu\text{g m}^{-3}$) of Benzene, Toluene and SO₂.

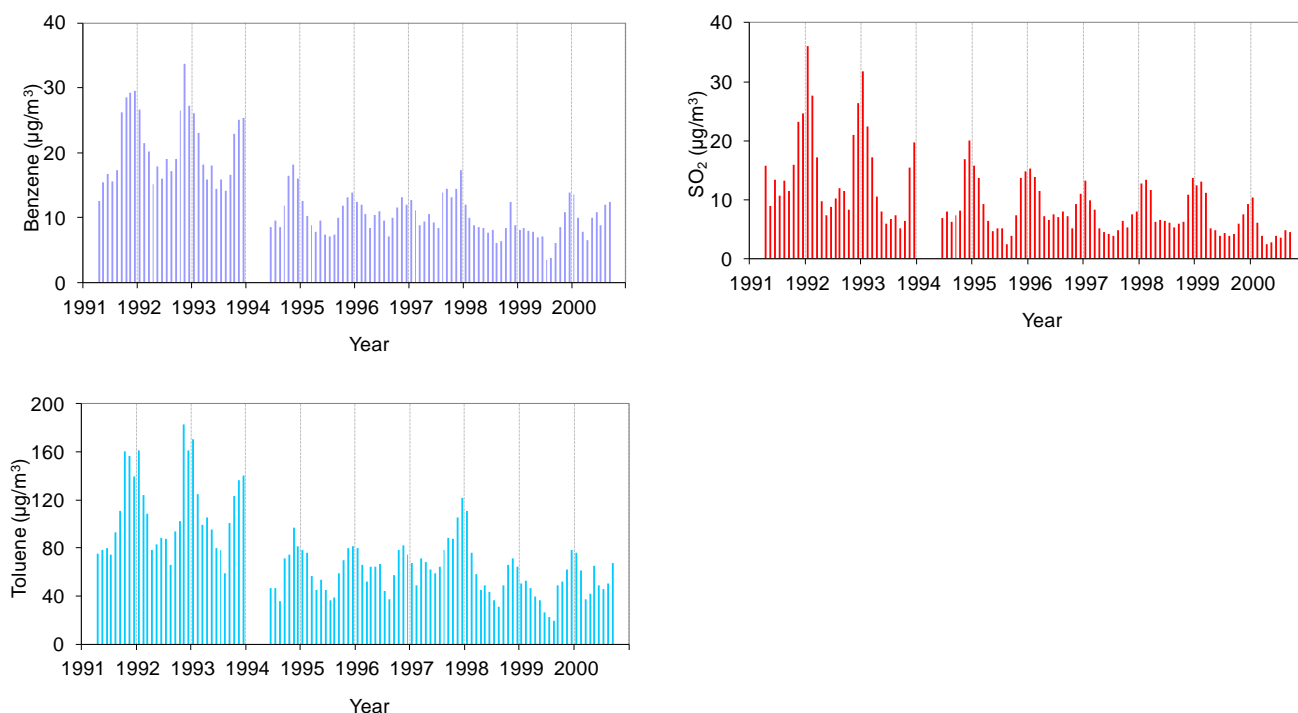


Figure 4. Primary pollutants: monthly trends of the month average concentration ($\mu\text{g m}^{-3}$) of Benzene, Toluene and SO₂.

For secondary pollutants, such as ozone, nitrogen dioxide, nitrous acid and formaldehyde (Figure 5), no clear trend can be recognized looking at their average annual concentrations, because they are

not directly related to the sources of pollution. Their pattern of variation is determined both by the atmospheric stability conditions and by the pool of reactions involving O_3 , NO_x , NMHCs and UV radiation.

As regards ozone, in summer its concentrations are higher than in the rest of the year, due to the higher photochemical activity in this period. On the other hand, nitrogen dioxide exhibits a complementary trend to the O_3 one (Figure 6).

Both primary sources (i.e. direct emissions from anthropogenic sources) and secondary sources (i.e. production in the atmosphere during oxidation of other, directly emitted NMHCs) contribute to atmospheric concentrations of HCHO. Most secondary production of HCHO occurs during the atmospheric oxidation of ethene, propene and higher terminal alkenes, such as 1-butene, 1,3-butadiene and isoprene, but HCHO is additionally formed more slowly from the oxidation of alkanes and aromatic compounds [51-53].

HNO_2 is a pollutant formed during the first hours of the morning for heterogeneous reaction of NO_2 with H_2O [54,55]. HNO_2 in the lower atmosphere derives from direct emissions (motor vehicle exhaust) or chemical formation. Chemical sources include the gas-phase formation from the reaction between OH and nitric oxide (NO) and heterogeneous formation on surfaces from NO_2 hydrolysis.

For these two pollutants, the trends are generally decreasing in the summer period, thanks to meteorological conditions favoring their dispersion, due to convective mixing. In addition, in summer, because of prolonged periods of solar radiation, HNO_2 photodissociates itself producing OH radicals. Instead, in winter the two pollutants display an increasing trend for the contribution of the domestic heating and the reduction of the mixing height [56-58].

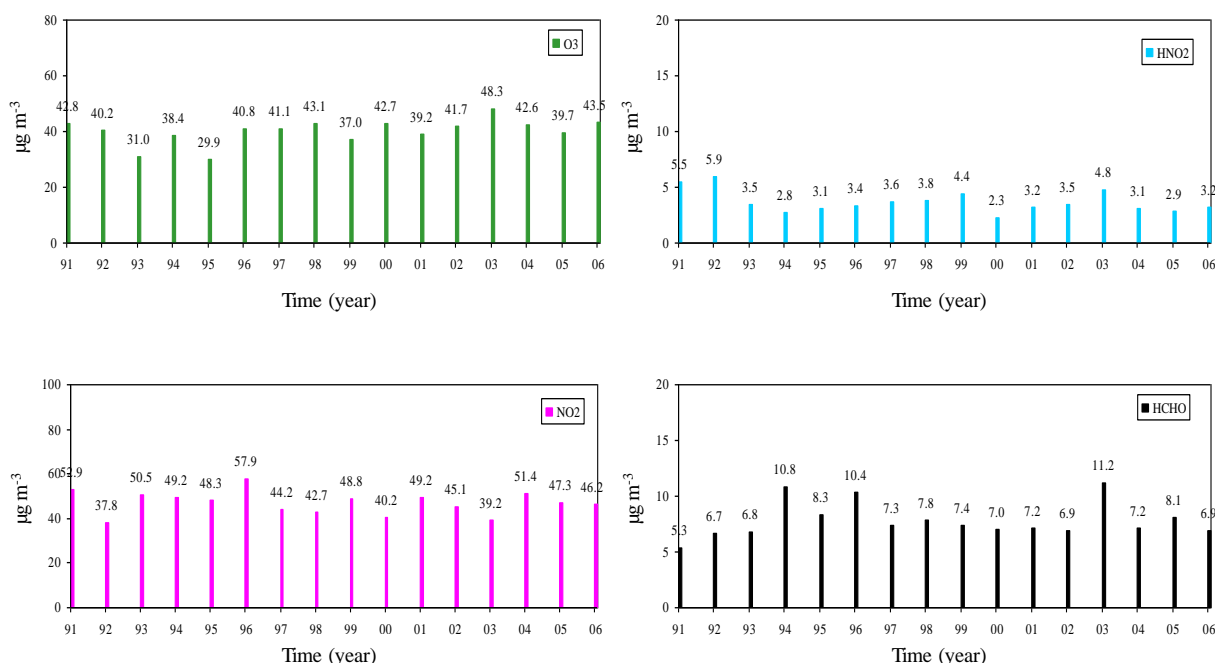


Figure 5. Secondary pollutants: annual trends of the month average concentration ($\mu\text{g m}^{-3}$) of Ozone, NO_2 , Nitrous acid and Formaldehyde.

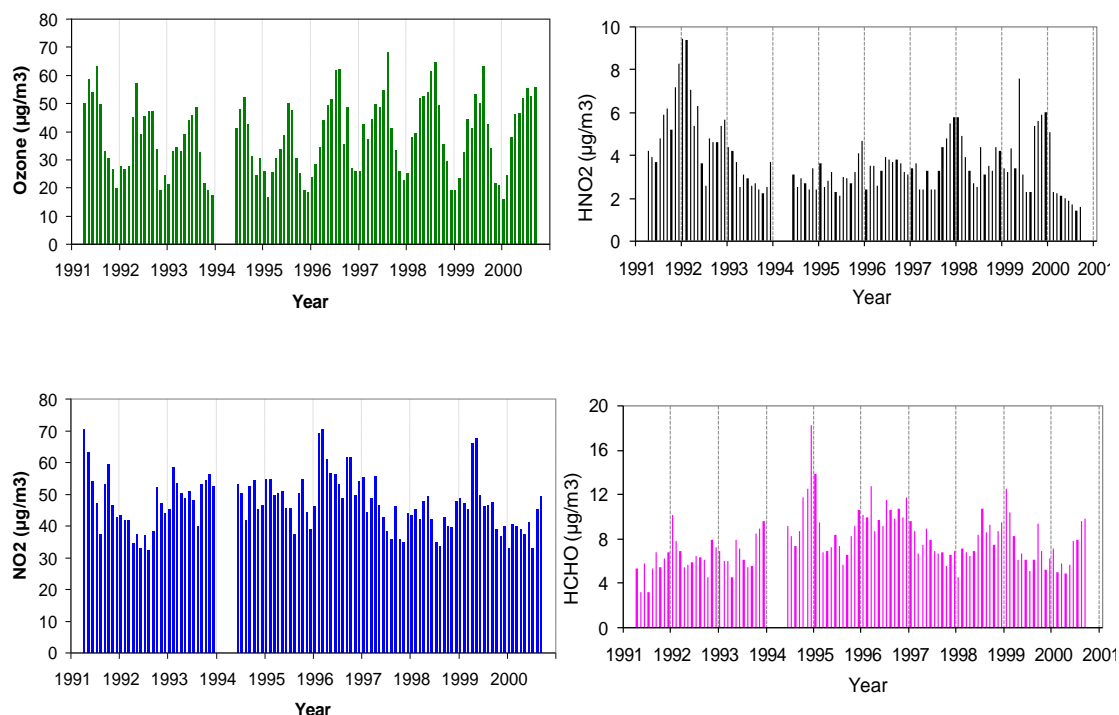


Figure 6. Secondary pollutants: monthly trends of the month average concentration ($\mu\text{g m}^{-3}$) of Ozone, NO_2 , Nitrous acid and Formaldehyde.

The occurrence of radical oxidative processes in atmosphere can be represented through the variable O_x , defined as the sum of O_3 and NO_2 concentrations.

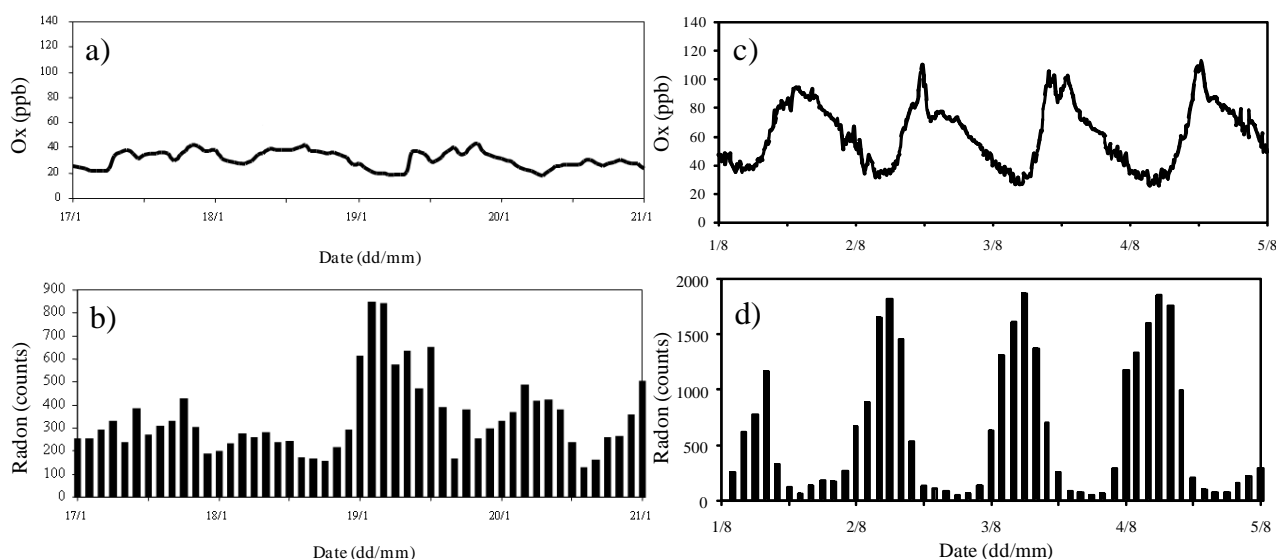


Figure 7. Dynamic of O_x variable in relationship to the meteorological conditions: O_x (a,c) and Radon (b,d) concentration trends during instability and stability conditions, respectively (downtown Rome, January and August 2012).

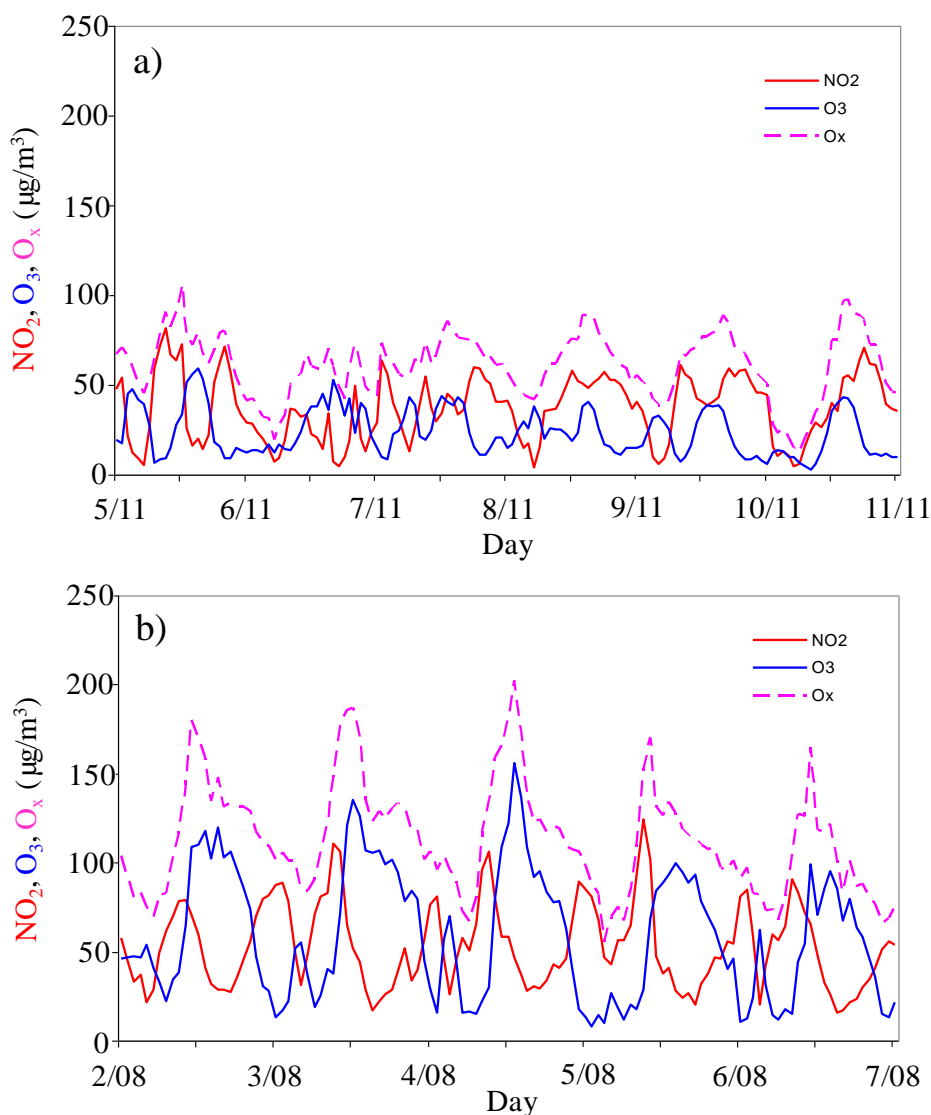


Figure 8. Ozone, NO₂ and O_x daily concentration trends during instability (a) and stability (b) conditions, respectively (downtown Rome, August 2013).

During periods of low photochemical activity and of high advection (Figure 7b), O_x is characterized by a trend fairly constant with oscillation around the background ozone value (Figure 7a). In this case a photostationary condition is reached, since ozone is mainly formed through the photolysis of NO₂ and decomposed by reaction with NO. Then, the two pollutants show a complementary pattern of variation (Figure 8a).

When the advective transport mechanism is negligible and during atmospheric stability periods (Figure 7d), radical oxidative processes may play an important role. O_x trend is very well structured (Figure 7c). It displays minimum values at night, almost due to NO₂, because the ozone concentrations are very low. Figure 8b shows that, because of the occurrence of radical oxidative processes, O₃ and NO₂ present a no more specular trend of variation.

During the day, peak values above the background value are indicative of radical oxidative activity. The radon concentration trend displays a peculiar modulation characterized by maximum values at night, due to nocturnal atmospheric stability, alternating with minimum values during the day,

due to convective mixing.

It is interesting to note that such pattern is complementary to the O_x one: minimum radon concentration value (high degree of mixing of the low atmospheric layer) correspond to maximum O_x values (high solar radiation and radical oxidative activity) and vice versa.

Taking into account that formaldehyde is also a secondary pollutant, Figure 9 shows that in correspondence of peak values of the variable O_x , indicative of radical oxidative activity, we observe also peaks of the formaldehyde concentration, clearly of secondary origin.

Finally, a final consideration should be devoted to the contribution of the airborne particulate matter to the photochemical activity. In particular, this pollutant is composed by two main fractions, carbonaceous and non-carbonaceous, and the carbonaceous part is more relevant than the second in the photochemical processes. In fact, the carbonaceous particulate matter (total carbon, TC) material is classified into elemental carbon (EC) or black carbon (BC), depending on its thermal or optical properties respectively, and organic carbon (OC). The EC fraction has a graphitic structure: it is a primary pollutant emitted directly during the combustion processes

The OC fraction is composed by different classes of compounds (hydrocarbons, oxygenated hydrocarbons, etc.): it has both primary and secondary origins [59,60]. The primary OC is emitted as sub-micron particles or from biogenic plant emission, whereas the secondary OC can have origin from gas-particle NMHC condensation with low vapor pressure, by chemical-physical adsorption of gaseous species on particles or as product from photochemical atmospheric reactions [61].

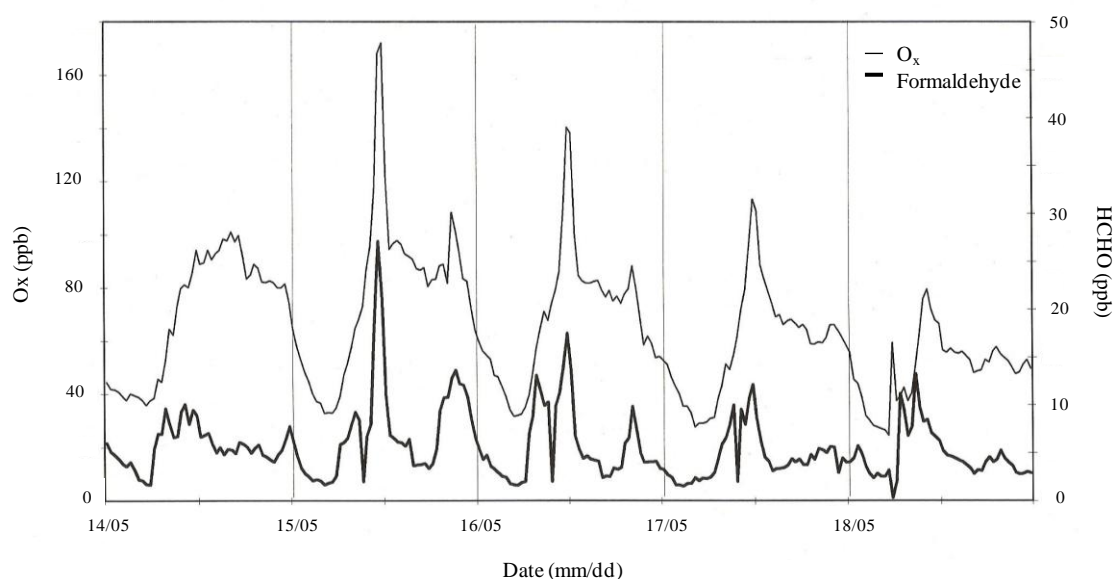


Figure 9. Formaldehyde and O_x daily concentration trends during instability and stability conditions (downtown Rome, May 2011).

The correlation (Figure 10) observed between OC and EC, good in winter and less good in summer, suggests that in the urban area of Rome the carbonaceous PM pollution is of primary origin, with an important contribution of secondary organic carbon in summer, particularly during high photochemical activity periods.

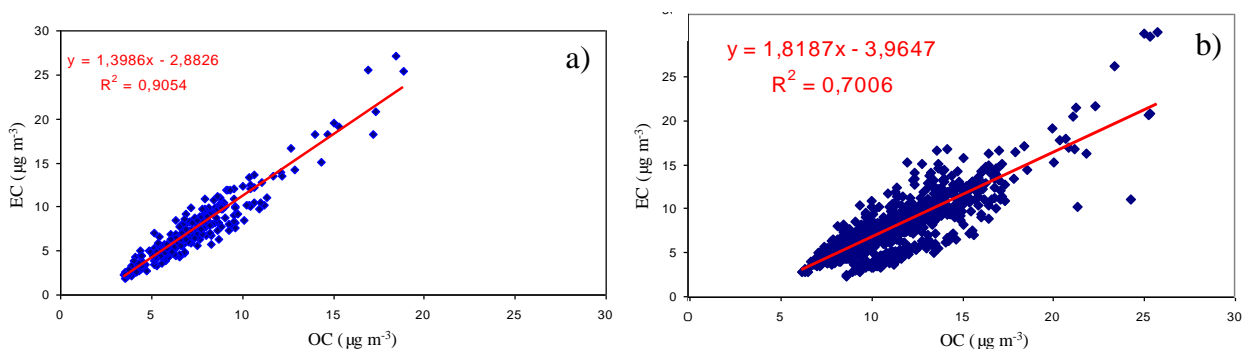


Figure 10. Organic Carbon vs. Elemental Carbon correlations in winter (a) and summer (b) periods (downtown Rome, 2012).

Figure 11 shows an O_x variation pattern very well structured, suggestive of a strong radical oxidative process during the day. Coherently, the TC to EC ratio increases from about 2 to about 3, thanks to photochemical reactions leading to the formation of secondary organic carbon.

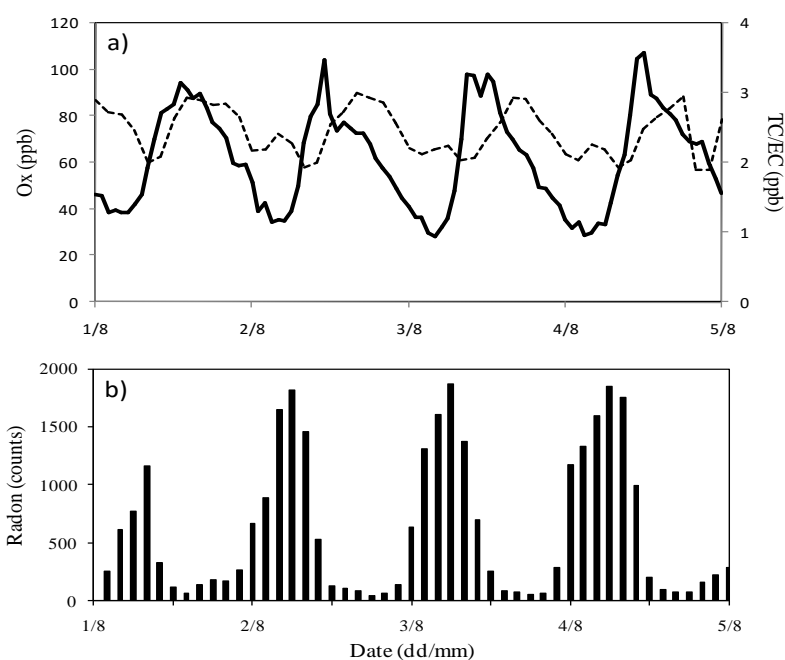


Figure 11. Daily trends of TC/EC ratio and O_x variable ($= NO_2 + O_3$) (a) vs. Radon concentration trend (b) (downtown Rome, August 2012).

In urban air, due to anthropogenic phenomena such as combustion and/or domestic heating, the No-Methane Hydrocarbons (NMHCs) are a very significant component: some of them are considered toxic air contaminants (benzene) or harmful (toluene, xylenes).

NMHCs play a key role in the formation of photochemical processes [62,63]: in fact, they are considered precursors for the ozone production at ground level when conditions of solar radiation and nitrogen oxides are “favorable”. The ozone at ground level, usually considered “bad ozone”, can seriously damage the environment and the human health. The NMHCs and aromatic ones, participating in the formation of photochemical smog in urban and suburban areas, strongly influence,

with different percentages, the total ozone concentration [64]. Derwent and Jenkin [65] were the first to determine that *m*-xylene, trimethylbenzene and C₃–C₄ alkenes produce more ozone than ethylene. After, other authors have highlighted the reactivity of many potentially toxic and mutagenic substances in atmosphere.

Table 1 summarizes the arithmetic means concentrations of hydrocarbons C₁–C₇ and aromatic compounds in the air of Mexico City [66] and Rome. Rome data are related to only one location (downtown Rome) in March whereas the literature data are related to samplings performed throughout Mexico City both during different days, different hours and different locations [66] but, also in this case, the values reported in Table 1 are the arithmetic means.

Table 1. Concentration levels ($\mu\text{g m}^{-3}$) of methane, NMHCs including aromatic compounds in Rome and Mexico City [66] along with the relative percentage contributions of each compound to the ozone formation.

	Level ($\mu\text{g m}^{-3}$)		Contribution (%)	
	Rome	Mexico City	Rome	Mexico City
Methane	1329	1732	2.6	1.3
Ethane	10.9	17.2	0.4	0.2
Propane	10.8	285.0	0.7	6.8
<i>n</i> -Butane	10.5	167.3	1.4	8.5
iso-Butane	6.2	78.7	1.0	4.7
<i>n</i> -Pentane	5.3	42.5	0.7	2.2
iso-Pentane	18.9	57.5	3.4	3.9
<i>n</i> -Heptane	14.5	43.4	1.9	2.1
2-Methylpentane	7.8	28.6	1.6	2.2
3-Methylpentane	5.6	18.7	1.1	1.4
<i>n</i> -Heptane	2.0	13.7	0.2	0.6
Ethylene	8.4	24.9	8.2	9.1
Propene	4.8	8.6	6.0	4.0
1-Butene	0.9	4.9	1.2	2.2
<i>i</i> -Butene	1.4	4.1	0.9	1.1
<i>trans</i> -2-Butene	0.7	3.0	1.0	1.5
<i>cis</i> -2-Butene	0.7	3.2	1.0	1.6
1-Pentene	0.0	1.1	0.0	0.3
<i>n</i> -Hexane	0.3	1.4	0.2	0.3
Acetylene	9.7	33.7	0.6	0.8
1,3-Butadiene	0.4	0.9	0.8	0.5
Isoprene	1.7	0.3	2.1	0.2
Benzene	11.5	15.0	0.6	0.3
Toluene	35.0	79.1	12.6	10.7
<i>o</i> -Xylene	9.1	10.9	7.6	3.5
<i>m</i> -Xylene	16.5	26.1	18.0	10.6
<i>p</i> -Xylene	6.5	10.0	5.6	3.3
Ethyl benzene	7.8	20.8	2.7	2.8
Styrene	0.4	2.6	0.2	0.3
1,3,5-trimethylbenzene	2.9	13.8	3.6	6.9
1,2,4-trimethylbenzene	10.3	13.8	11.9	6.0

Looking at the concentrations of ethane ($10.9 \mu\text{g m}^{-3}$), acetylene ($9.7 \mu\text{g m}^{-3}$) and *i*-pentane (18.9

$\mu\text{g m}^{-3}$), it is confirmed the evidence of an impact of the incomplete combustion (fuel/diesel exhaust) from autovehicular traffic in downtown Rome along with fuel evaporation, biogenic, LPG and evaporative emissions that play an important role in urban area [21,63].

Regarding Mexico City [66], the concentrations of propane, *n*-butane and *i*-butane are significantly higher than those found in Rome; the toluene/benzene ratio ranges from 1.3 in rural area 50 km north-east of Mexico City to 5.1 in downtown Mexico City at rush hour, with an average level of 5.3 for all the data-set [66]. About the value in rural area, the value can be due to traffic emissions as the air masses could have been transported from traffic sources and photochemically processed causing a depletion of toluene vs. benzene [67]: however, unfortunately [66] did not give more information, neither about the sampling site nor meteorological conditions.

It should be underlined that the ratio (based on mixing ratio units) of toluene and benzene (3.12 ± 0.22) is on average in agreement with that previously measured in urban areas in Rome characterized by vehicle traffic (ratio between 3 and 5) [68] whereas is higher than the ratio determined in other cities [69]. The large ratio variation could essentially be due to the different fuels (among them, there was leaded and unleaded gasoline) available on the Italian market, with different content of aromatic hydrocarbons.

Further, in Table 1, for each hydrocarbon analyzed the contribution to the ozone formation, according to the method of the Maximum Incremental Reactivity (MIR) developed by Carter, was calculated [64].

The *m*-xylene, toluene and 1,2,4-TMB show major contributions to ozone formation. Comparing the data of Rome with those of Mexico City, it can be noted the same contribution from toluene (12.6% in Rome and 10.7% in Mexico City), a higher contribution of *m*-xylene (18.0% in Rome and 10.6% in Mexico City) and a significant percentage of 1,2,4-TMB (11.9% in Rome instead of 6.0% of Mexico City).

In particular, for *m*-xylene and 1,2,4-TMB, this contribution is mainly due to their greater Maximum Incremental Reactivity (MIR), rather than to their concentrations ($16.5 \mu\text{g m}^{-3}$ and $10.3 \mu\text{g m}^{-3}$, respectively), which are relatively similar, e.g., ethane ($10.9 \mu\text{g m}^{-3}$), which contributes negligibly to the ozone formation (0.4%).

4. Conclusion

In the last decades, we have observed a decreasing trend of some primary pollutant, in particular, as regards their photochemical potential to produce O_3 , of benzene and toluene. Ozone is a secondary pollutant: its formation requires the concomitant presence of solar radiation (that promote photochemical reaction), NO_x (that through the photolysis of NO_2 release atomic oxygen) reactive NMHCs (that open the photostationary cycle involving O_3 and NO_x). Then, the control of O_3 atmospheric concentration passes through the control of its precursors. The variable O_x is a useful parameter to detect the occurrence of radical oxidative processes in atmosphere. Such process can lead to the formation of secondary OC particulate matter. Radon and its short-lived decay products can be assumed as a valuable indicator of the mixing degree of the low atmospheric layer.

This work also shows for the first time the percentage contribution of each Non-Methane Hydrocarbon to the ground-level ozone formation in downtown Rome and the relative data are compared with those found for Mexico City. Based on the toluene/benzene ratios found in downtown Rome and for various sites in Mexico City, also in the case of downtown Rome as for Mexico City the autovehicular traffic is likely an important source of ozone precursors, albeit some cities like Mexico

City may have additional significant NMHC sources. In general, the main contributors to ozone formation in downtown Rome are due to aromatic hydrocarbons (62.8%) and alkenes (21.4%).

Acknowledgments

This study was supported by the INAIL grants P20L01 and P20L09.

Conflict of Interest

The authors declare no conflict of interest.

References

1. Filanyson-Pitts BJ, Pitts JN Jr (1986) *Atmospheric Chemistry Fundamentals and Experimental Techniques*, New York: Wiley.
2. Olaguer EP, Rappenglück B, Lefer B, et al. (2009) Deciphering the role of radical sources during the Second Texas Air Quality Study. *J Air Waste Man Assoc* 59: 1258-1277.
3. Rappenglück B, Oyola P, Olaeta I, et al. (2000) The evolution of photochemical smog in the Metropolitan Area of Santiago de Chile. *J Appl Meteor* 39: 275-290.
4. Rappenglück B, Schmitza R, Bauerfeind M, et al. (2005) An urban photochemistry study in Santiago de Chile. *Atmos Environ* 39: 2913-2931.
5. Czader BH, Byuna DW, Kima S-T (2008) A study of VOC reactivity in the Houston-Galveston air mixture utilizing an extended version of SAPRC-99 chemical mechanism. *Atmos Environ* 42: 5733-5742.
6. Paulson SE, Orlando JJ (1996) The reactions of ozone with alkenes: an important source of HOx in the boundary layer. *Geophys Res Lett* 23: 3727-3730.
7. Wolff S, Boddenberg A, Thamm J, et al. (1997) Gas-phase ozonolysis of ethene in the presence of carbonyl-oxide scavengers. *Atmos Environ* 31: 2965-2969.
8. Osborn DL, Hyeon C, Mordaunt DH, et al. (1997) Fast beam photodissociation spectroscopy and dynamics of the vinoxy radical. *J Chem Phys* 106: 3049-3066.
9. Calvert JG, Atkinson R, Kerr JA, et al. (2000) *The Mechanism of atmospheric oxidation of the alkenes*. Oxford University Press, New York.
10. Ryerson TB, Trainer M, Angevine WM, et al. (2003) Effect of petrochemical industrial emissions of reactive alkenes and NOx on tropospheric ozone formation in Houston, Texas. *J Geophys Res* 108: 4249-4273.
11. Chan WT, Hamilton IP (2003) Mechanisms for the ozonolysis of ethene and propene: Reliability of quantum chemical predictions. *J Chem Phys* 118: 1688-1701.
12. Topaloglou C, Kazadzis S, Bais AF, et al. (2005) NO₂ and HCHO photolysis frequencies from irradiance measurements in Thessaloniki, Greece. *Atmos Chem Phys* 5: 1645-1653.
13. Johnson D, Marston G (2008) The gas-phase ozonolysis of unsaturated volatile organic compounds in the troposphere. *Chem Soc Rev* 37: 699-716.
14. Volkamer R, Sheehy P, Molina LT, et al. (2010) Oxidative capacity of the Mexico City atmosphere - Part 1: A radical source perspective. *Atmos Chem Phys* 10: 969-991.
15. Su H, Cheng Y, Oswald R, et al. (2011) Soil nitrite as a source of atmospheric HONO and OH radicals. *Science* 333: 1616-1618.

16. Alam MS (2011) Total radical production and degradation products from alkene ozonolysis. Ph.D. Thesis (available at http://theses.bham.ac.uk/1733/2/Alam_11_PhD.pdf; accessed on May 2015).
17. Alam MS, Camredon M, Rickard AR, et al. (2011) Total radical yields from tropospheric ethene ozonolysis. *Phys Chem Chem Phys* 13: 11002-11015.
18. Edwards PM, Young CJ, Aikin K, et al. (2013) Ozone photochemistry in an oil and natural gas extraction region during winter: simulations of a snow-free season in the Uintah Basin, Utah. *Atmos Chem Phys* 13: 8955-8971.
19. Vrekoussis M, Mihalopoulos N, Gerasopoulos N, et al. (2007) Two-years of NO₃ radical observations in the boundary layer over the Eastern Mediterranean. *Atmos Chem Phys* 7: 315-327.
20. Rollins AW, Kiendler-Scharr A, Fry J, et al. (2009) Isoprene oxidation by nitrate radical: alkyl nitrate and secondary organic aerosol yields. *Atmos Chem Phys* 9: 6685-6703.
21. Jorquera H, Rappenglück B (2004) Receptor modeling of ambient VOC at Santiago, Chile. *Atmos Environ* 38: 4243-4263.
22. Elshorbany YF, Kurtenbach R, Wiesen P, et al. (2009) Oxidation capacity of the city air of Santiago, Chile. *Atmos Chem Phys* 9: 2257-2273.
23. Elshorbany YF, Kleffmann J, Kurtenbach R, et al. (2009) Summertime photochemical ozone formation in Santiago, Chile. *Atmos Environ* 43: 6398-6407.
24. Czader BH, Li X, Rappenglück B (2013) CMAQ modeling and analysis of radicals, radical precursors, and chemical transformations. *J Geophys Res* 118: 11376-11387.
25. Czader BH, Rappenglück B (2015) Modeling of 1,3-butadiene in urban and industrial areas. *Atmos Environ* 102: 30-42.
26. Riedel TP, Wolfe GM, Danas KT, et al. (2014) An MCM modeling study of nitryl chloride (ClNO₂) impacts on oxidation, ozone production and nitrogen oxide partitioning in polluted continental flow. *Atmos Chem Phys* 14: 3789-3800.
27. Mao J, Rena X, Chen S, et al. (2010) Atmospheric oxidation capacity in the summer of Houston 2006: comparison with summer measurements in other metropolitan studies. *Atmos Environ* 44: 4107-4115.
28. Elshorbany YF, Kleffmann J, Kurtenbach R, et al. (2010) Seasonal dependence of the oxidation capacity of the city of Santiago de Chile. *Atmos Environ* 44: 5383-5394.
29. European Commission, Directive 2008/50/EC of the European Parliament and of the Council of 21 May 2008 on ambient air quality and cleaner air for Europe. 2008. Available from: <http://eur-lex.europa.eu/legal-content/EN/TXT/?uri=celex:32008L0050#text>
30. Mustafa MG (1990) Biochemical basis of ozone toxicity. *Free Radical Biol Med* 9: 245-265.
31. Hazuchaa MJ, Lefohn AS (2007) Nonlinearity in human health response to ozone: experimental laboratory considerations. *Atmos Environ* 41: 4559-4570.
32. Pryor WA, Squadrito GL, Friedman M (1995) The cascade mechanism to explain ozone toxicity: the role of lipid ozonation products. *Free Radical Biol Med* 19: 935-941.
33. Stockinger HE (1965) Ozone toxicology: a review of research and industrial experience. *Arch Environ Health* 10: 719-731.
34. Avino P, De Lisio V, Grassi M, et al. (2004) Influence of air pollution on Chronic Obstructive Respiratory Diseases: comparison between city (Rome) and hillcountry environments and climates. *Ann Chim (Rome)* 94: 629-636.

35. Ferretti M, Fagnano M, Amoriello T, et al. (2007) Measuring, modelling and testing ozone exposure, flux and effects on vegetation in southern European conditions - What does not work? A review from Italy. *Environ Poll* 146: 648-658.
36. Platt U, Perner D, Patz HW (1979) Simultaneous measurement of atmospheric CH₂O, O₃ and NO₂ by differential optical absorption. *J Geophys Res* 84: 6329-6335.
37. Morales JA, Treacy J, Coffey S (2004) Urban ozone measurements using differential optical absorption spectroscopy. *Anal Bioanal Chem* 379, 51-55.
38. Avino P, Manigrasso M (2008) Ten-year measurements of gaseous pollutants in urban air by an open-path analyzer. *Atmos Environ* 42: 4138-4148.
39. Avino P, Brocco D, Lepore L (2001) Determination of atmospheric organic and elemental carbon particle in Rome with a thermal method. *Anal Lett* 34: 967-974.
40. Avino P, Brocco D, Cecinato A, et al. (2002) Carbonaceous component in atmospheric aerosol: measurement procedures and characterization. *Ann Chim (Rome)* 92: 333-341.
41. Avino P, Brocco D, Lepore L, et al. (2000) Distribution of elemental carbon (EC) and organic carbon (OC) in the atmospheric aerosol particles of Rome. *J Aerosol Sci* 31: S364-S365.
42. Avino P, Brocco D, Lepore L, et al. (2003) Interpretation of atmospheric pollution phenomena in relationship with the vertical atmospheric remixing by means of natural radioactivity measurements (Radon) of particulate matter. *Ann Chim (Rome)* 93: 589-594.
43. Febo A, Guglielmi F, Manigrasso M, et al. (2010) Local air pollution and long-range mass transport of atmospheric particulate matter: a comparative study of the temporal evolution of the aerosol size fractions. *Atmos Poll Res* 1: 141-146.
44. Manigrasso M, Febo A, Guglielmi F, et al. (2012) Relevance of aerosol size spectrum analysis as support to qualitative source apportionment studies. *Environ Poll* 170: 43-51.
45. Avino P, Manigrasso M, Cuomo F (2015) Natural radioactivity as an easy and quick parameter for describing the dynamic of the Planetary Boundary Layer. *RSC Adv* 5: 57538-57549.
46. Law n. 413 of 04/11/1997. Misure urgenti per la prevenzione dell'inquinamento atmosferico da benzene. *Gazzetta Ufficiale Italiana* n. 282 of 03/12/1997.
47. Rappenglück B, Lubertino G, Alvarez S, et al. (2013) Radical precursors and related species from traffic as observed and modeled at an urban highway junction. *J Air Waste Man Assoc* 63: 1270-1286.
48. Monod A, Sive BC, Avino P (2001) Monoaromatic compounds in ambient air of various cities: a focus on correlations between the Xylenes and Ethylbenzene. *Atmos Environ* 35: 135-149.
49. De Lauretis R, Ilacqua M, Romano D (2003) Emissioni di benzene in Italia dal 1990 al 2000. Rapporti X/2003. APAT-Dipartimento Stato dell'Ambiente, Controlli e Sistemi Informativi-Unita Interdipartimentale Censimento Fonti di Emissione.
50. Council Directive 93/12/EEC of 23 March 1993 relating to the sulphur content of certain liquid fuels and Council Directive 98/70/EC of the European Parliament and of the Council of 13 October 1998 relating to the quality of petrol and diesel fuels and amending Council Directive 93/12/EEC.
51. Rappenglück B, Dasgupta PK, Leuchner M, et al. (2010) Formaldehyde and its relation to CO, PAN, and SO₂ in the Houston-Galveston airshed. *Atmos Chem Phys* 10: 2413-2424.
52. Movassaghi K, Russo MV, Avino P (2012) The determination and role of peroxyacetyl nitrate in photochemical processes in atmosphere. *Chem Central J* 6: S8.
53. Parrish DD, Ryerson TB, Mellqvist J, et al. (2012) Primary and secondary sources of formaldehyde in urban atmospheres: Houston Texas region. *Atmos Chem Phys* 12: 3273-3288.

54. Febo A, Perrino C, Bruno P, et al. (1999) Formation and occurrence of nitrous acid in the atmosphere (FORMONA), Final report to the European Commission (ENV4-CT95-0055). Consiglio Nazionale delle Ricerche, Rome.
55. Czader BH, Rappenglück B, Percell P (2012) Modeling nitrous acid and its impact on ozone and hydroxyl radical during the Texas Air Quality Study 2006. *Atmos Chem Phys* 12: 6939-6951.
56. Wiesen P (2002) Nitrous acid and its influence on the oxidation capacity of the atmosphere (NITROCAT), final EU project report (EVK2-CT-1999-00025).
57. Acker K, Möller D, Auel R, et al. (2005) Concentrations of nitrous acid, nitric acid, nitrite and nitrate in the gas and aerosol phase at a site in the emission zone during ECOMPTE 2001 experiment. *Atmos Res* 74: 507-524.
58. Acker K, Febo A, Trick, et al. (2006) Nitrous acid in the urban area of Rome. *Atmos Environ* 40: 3123-3133.
59. Heintzenberg J (1982) Size-segregated measurements of particulate elemental carbon and aerosol light absorption at remote locations. *Atmos Environ* 16: 2461-2469.
60. Avino P, Brocco D, Pareti S, Scalisi G (2003) Description of the carbonaceous particulate matter evolution in an urban area. *Ann Chim* 93: 21-26.
61. Avino P, Manigrasso M, Rosada A, et al. (2015) Measurement of organic and elemental carbon in downtown Rome and background area: physical behavior and chemical speciation. *Environ Sci Process Impacts* 17: 300-315.
62. Kourtidis KA, Ziomasa IC, Rappenglück B, et al. (1999) Evaporative traffic hydrocarbon emissions, traffic CO and speciated HC traffic emissions from the city of Athens. *Atmos Environ* 33: 3831-3842.
63. Leuchner M, Rappenglück B (2010) VOC source-receptor relationships in Houston during TexAQS-II. *Atmos Environ* 44: 4056-4067.
64. Carter WPL (1994) Development of ozone reactivity scales for volatile organic compounds. *J Air Waste Manage* 44: 881-899.
65. Derwent RG, Jenkin ME (1991) Hydrocarbons and the long-range transport of Ozone and PAN across Europe. *Atmos Environ* 25A: 1661-1678.
66. Blake DR, Rowland FS (1995) Urban leakage of liquefied petroleum gas and its impact on Mexico City air quality. *Science* 269: 953-956.
67. Winkler J, Blank P, Glaser K, et al. (2002) Ground-based and airborne measurements of nonmethane hydrocarbons in BERLIOZ: analysis and selected results. *J Atmos Chem* 42: 465-492.
68. Brocco D, Fratarcangeli R, Lepore L, et al. (1997) Determination of aromatic hydrocarbons in urban air of Rome. *Atmos Environ* 21: 557-566.
69. Rappenglück B, Fabian P (1999) Nonmethane hydrocarbons (NMHC) in the Greater Munich Area/Germany. *Atmos Environ* 33: 3843-3857.



AIMS Press

© 2015 Pasquale Avino, et al., licensee AIMS Press. This is an open access article distributed under the terms of the Creative Commons Attribution License (<http://creativecommons.org/licenses/by/4.0>)